Synthesis and Characterization of Fe-Al_2O_3 Nanoparticles Prepared by Coprecipitation Method

Farahmandjou, Majid*+
Department of Physics, Varamin Pishva Branch, Islamic Azad University, Varamin, I.R. IRAN

Khodadadi, Abolfazl
Department of Physics, Tehran North Branch, Islamic Azad University, Tehran, I.R. IRAN

Yaghoubi, Mojtaba
Departments of Physics, Islamic Azad University, Ayatollah Amoli Branch, Amol, I.R. IRAN

Khodadadi, Shahaab
Department of Science, Tehran Medical Branch, Islamic Azad University, Tehran, I.R. IRAN

ABSTRACT: *In this study, iron-doped alumina (Fe-Al_2O_3) nanoparticles (NPs) containing 2 mol%, 4 mol%, and 6 mol% iron impurities were fabricated by the co-precipitation method in the presence of $Al_2(SO_4)_3.9H_2O$ and $Fe_2(SO_4)_3.9H_2O$ precursors. The prepared nanoparticles were heated at 1000 ºC to study their physicochemical properties. The XRD results pointed out the multiphase for the samples. The morphological results revealed that the uniformity increased by increasing iron atoms rate. TEM analysis revealed that the particle with a size of 40 nm was obtained for 4% of the sample. The results of FT-IR analysis indicated that when the 2% impurity increases the AlO_4 tetrahedra and AlO_6 octahedral vibrational bond grow.*

KEYWORDS: *Fe-doped Al_2O_3; Nanocrystals; Coprecipitation method; Optical properties; Catalyst; Ceramics materials.*

INTRODUCTION

Metal oxide nanomaterials have been broadly considered in the fields of industry and medicine [1-22]. More specifically, the aluminum oxide NPs (alumina) have been extensively applied in electronics, optoelectronics, medicine, and petrochemical industries [23-29]. The properties of these nanomaterials are meaningfully changing by increasing the surface-to-volume ratio. Alumina has different phases of γ, η, κ, δ, θ, and α. The γ-phase has a cubic structure made at 700 to 1000 °C and is used generally as a catalyst and catalyst protector in structural and industrial composites and ceramic industry, whereas α phase has a hexagonal (hcp) structure and is formed when the heat increases to 1200°C. This structure is applied in the drilling and cutting subtle stones due to its high

*** To whom correspondence should be addressed.**
+ E-mail: farahmandjou@iauvaramin.ac.ir
1021-9986/2021/3/725-730 6/$/5.06

stiffness. The other phases are thermodynamically unstable whose structure eventually changes to the α-alumina phase when impurity is imbued and heat increases [30]. The α-Al_2O_3 unit cell has a hexagonal cell structure, having a rhombohedral primitive cell holding the atom. Each Al^{3+} center is in octagonal structure where Al^{3+} ions occupy two-third of the octagonal empty spaces in terms of crystallographic. The increase in temperature of alumina results in the loss of the hydroxyl group and the formation of Al^{4+} aluminum alpha cations in tetrahedral and Al^{6+} in octahedral, which in turn leads to phase transformation, porosity reduction, decrease in surface area, and an increase in size [31]. When a small amount of transition metal impurities such as Cu, Zn, and Fe is added, the crystalline, morphological, and optical properties of alumina NPs such as stiffness, crystalline order, and band gap are developed [32,33]. Due to the presence of an atomic radius close to Al (a_{Al3+}=0.57 Å), Fe (a_{Fe3+} =0.64 Å) dopant affects the physical properties of alumina more than the other transition metals [34]. Different methods such as the solgel process, hydrothermal, and co-precipitation methods are used to construct alumina NPs [35-37]. Among these methods, the co-precipitation method is more considered since it is reflected as an easy and economical synthesis and has better control over the formation and growth of NPs when compared to other methods [38,39]. In this investigation, pure alumina and impure alumina containing Fe impurity are synthesized by $Al_2(SO_4)_3.9H_2O$ and $Fe_2(SO_4)_3.9H_2O$ precursors with different Fe percentages of impurities using co-precipitation method. The impurity effects on crystalline and morphological properties of alumina are studied.

EXPERIMENTAL METHOD

Pure alumina and Fe-doped Al_2O_3 NPs with the precursors of $Al_2(SO_4)_3.9H_2O$ and $Fe_2(SO_4)_3.9H_2O$ were fabricated using co-precipitation approach. First, the defined amount of aluminum nitrate salt was dissolved in 100 ml of pure water. Then, the temperature was increased to 70 °C and then NaOH was slowly added and the heater temperature was then increased to 80 °C. To synthesize the Fe-doped alumina NPs with different percentages of 2%, 4%, and 6%, the defined amount of Iron nitrate salt was dissolved in 100 ml of dionized water. The samples were annealed at 1000 °C for 4 hours. Finally, nanoparticles

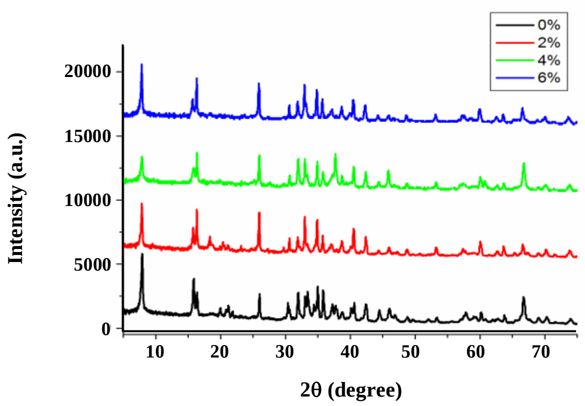

Fig. 1: XRD data of pure and Fe-doped alumina samples for different Fe dopants.

were analyzed to investigate the effect of iron doping in the alumina by XRD, FESEM, TEM and FTIR analyses.

RESULTS AND DISCUSSION

XRD Analysis

XRD spectra was carried out to characterize the NPs' crystal structure. Fig. 1 shows the XRD spectra of pure NPs and Fe-doped Al_2O_3 with different dopants of 2%, 4%, and 6%. The peaks at different angles representing the cubic structure in γ, δ, and the tetragonal structure of θ-alumina phase. Peaks created at 25.46, 35.23, 37.61, 41.05, 43.22, 45.63, 52.62, 57.43, 61.12, and 66.72 degrees are consistent with the diffraction Peaks at (012), (104), (110), (006), (113), (202), (024), (116), (122), and (214) indicating α-alumina phase with hexagonal structure [40].

FESEM Analysis

Fig. 2 shows the morphology of Fe-doped Al_2O_3 NPs with different dopants. Coating SEM samples with only a nm of Au increases the signal to noise ratio dramatically, resulting in crisp and clear images. As the figure illustrates, when iron impurities are added, the size of the NPs decreases, while their morphology increases. Actually, when the size decreases, the interatomic and molecular forces increase. Subsequently, NPs tend to be closer to each other resulting in their aggregation. The aggregation is resolved when the EG stabilizer is added to the sample [41-49]. The average calculated mean value for NPs with 57 nm in size and for impure NPs with 2%, 4%, and 6% impurities is equivalent to 51 nm, 49 nm, and 46 nm respectively.

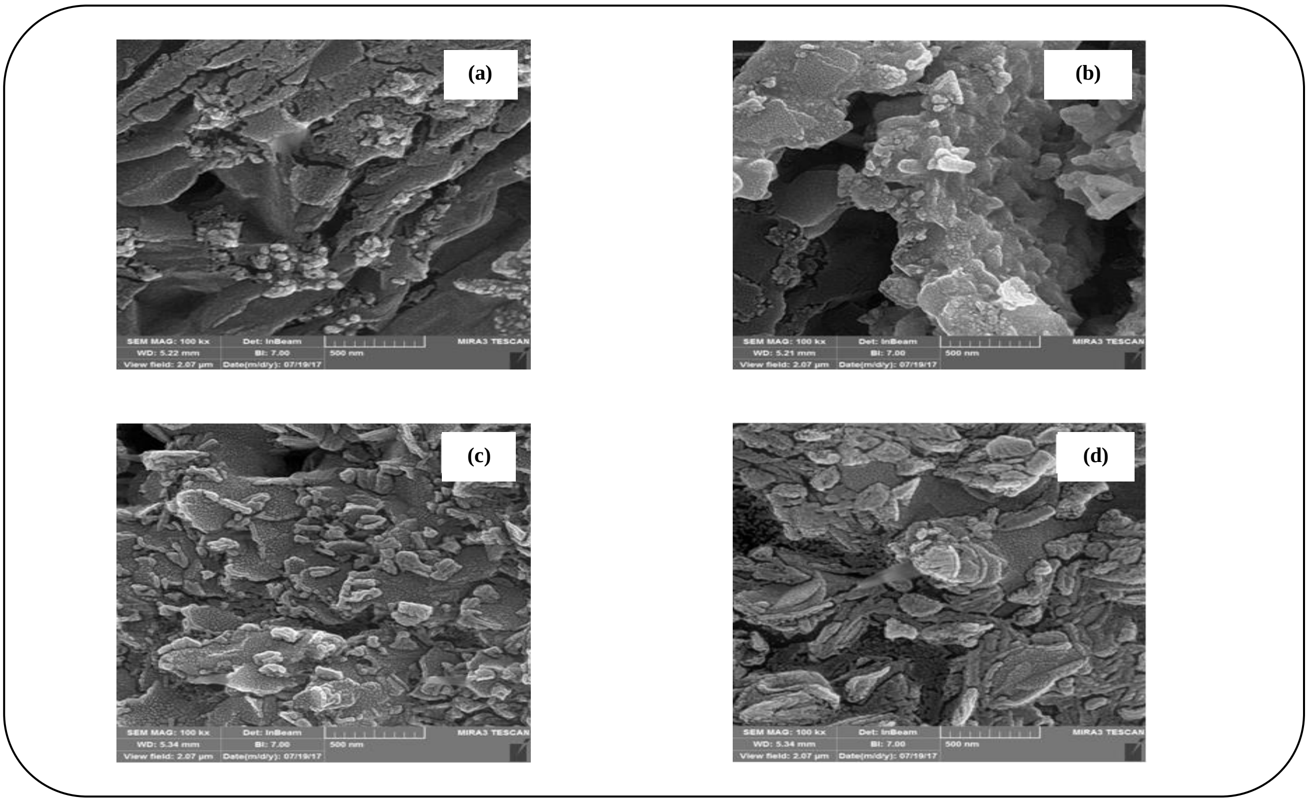

Fig. 2. FESEM images of (a) pure alumina, (b) 2%, (c) 4% and (d) 6% Fe-doped Al_2O_3.

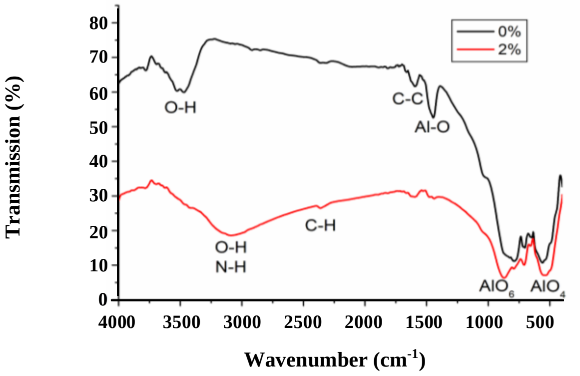

Fig. 3: FT-IR spectrum of the pure and 2% Fe-Al_2O_3 NPs..

FT-IR Analysis

To determine the functional groups and vibrational bond, Fourier Transform Infrared Spectroscopy (FT-IR) analysis was used. Fig. 3 indicates the transmission rate of pure and 2% Fe-doped alumina in terms of wave number. As it can be seen, the peaks in the frequency of 3078 cm^{-1} are associated with the O-H group. The peak generated in the wave number of 1589 cm^{-1} is related to C=C, and the vibrational peaks in the frequencies of 875 and 529 cm^{-1} are related to the tetrahedral and octahedral alumina groups, respectively. As it can be seen, the intensity of O-H adsorption increases with increasing Fe content which results the activation of OH^{o} radicals and increase in the catalytic activity [50].

TEM Analysis

To determine the exact size TEM analysis was used. The powders were dissolved by ethanol solution and dispersed by ultrasonic vibration for 30 minutes. As it can be seen in Fig. 4, the 4% Fe-doped alumina NPs are aggregated and their average size is measured to be 44.6 nm as measured by Gaussian fitting which is in agreement with XRD results. In fact, due to annealing process, the atomic interaction of the NPs increase and then the NPs form in a cluster [51-55].

CONCLUSIONS

Fe-doped Al_2O_3 NPs were successfully fabricated with Fe dopant percentages of 2%, 4%, and 6% using coprecipitation route. The XRD results pointed out that the

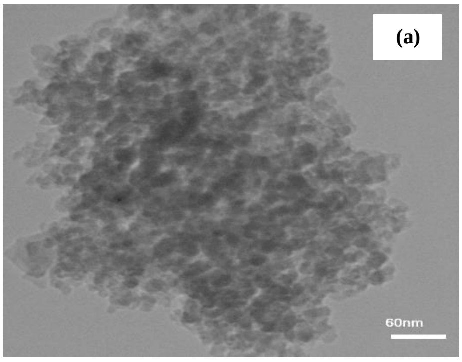

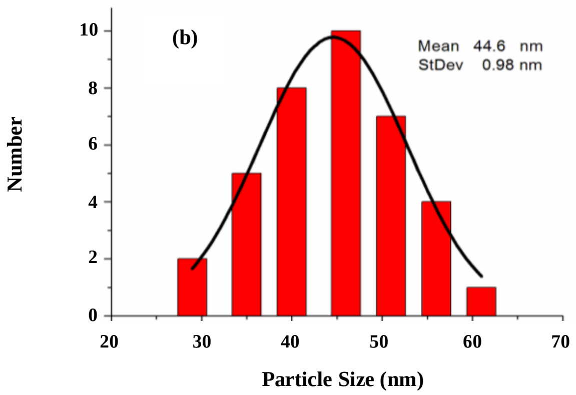

***Fig. 3:** FT-IR spectrum of the pure and 2% Fe-Al_2O_3 NPs..*

structure of the NPs is in multi-phasic form. The FESEM results revealed that when the dopant rate increases to 6%, the size of the NPs decreases to 46 nm. FTIR analysis shows increasing in Al-OH frequency due to increasing the Fe dopant of 2%.

Received : Aug. 19, 2019 ; Accepted : Jan. 13, 2020

REFERENCES

[1] Farahmandjou M., Ramazani M., Fabrication and Characterization of Rutile TiO_2 Nanocrystals by Water Soluble Precursor, *Phys. Chem. Res.*, 2015, **3**: 293-298 (2015).

[2] Shadrokh S., Farahmandjou M., Firozabadi T.P., Fabrication and Characterization of Nanoporous Co Oxide (Co_3O_4) Prepared by Simple Sol-gel Synthesis, *Phys. Chem. Res.*, **4**: 153-160 (2016).

[3] Farahmandjou M., Honarbakhsh S., Behrouzinia S., PVP-Assisted Synthesis of Cobalt Ferrite ($CoFe_2O_4$) Nanorods, *Phys. Chem. Res.*, **4**: 655-662 (2016).

[4] Dastpak M., Farahmandjou M., Firoozabadi T.P., Synthesis and Preparation of Magnetic Fe-doped CeO_2 Nanoparticles Prepared by Simple Sol-Gel Method, *J. Supercond. Nov. Magn.*, **29**: 2925-2929 (2016).

[5] Farahmandjou M., Soflaee F., Polymer-Mediated Synthesis of Iron Oxide (Fe_2O_3) Nanorods, *Chin. J. Phys.*, **53**: 080801-9 (2015).

[6] Jurablu S., Farahmandjou M., Firoozabadi T.P., Multiple-Layered Structure of Obelisk-Shaped Crystalline Nano-ZnO Prepared by Sol-Gel Route, *J. Theor. Appl. Phys.*, **9**: 261-266 (2015).

[7] Farahmandjou M., Soflaee F., Synthesis and Characterization of α-Fe_2O_3 Nanoparticles by Simple co-Precipitation Method, *Phys. Chem. Res.*, **3**: 193-198 (2015).

[8] Zarinkamar M., Farahmandjou M., Firoozabadi T.P., Diethylene Glycol-Mediated Synthesis of Nano-Sized Ceria (CeO_2) Catalyst, *J. Nanostruct.*, **6**: 116-120 (2016).

[9] Farahmandjou M., Magnetocrystalline Properties of Iron-Platinum ($L1_0$-FePt) Nanoparticles Through phase transition, *Iran. J. Phys. Res.*, **16**: 1-5 (2016).

[10] Farahmandjou M., Khalili P., Morphology Study of Anatase Nano-TiO_2 for Self-Cleaning Coating, *Int. J. Fund. Phys. Sci.*, **3**: 54-56 (2013).

[11] Farahmandjou M., Synthesis of ITO Nanoparticles Prepared by Degradation of Sulfide Method, *Chin. Phys. Lett.*, **29**: 077306-9 (2012).

[12] Farahmandjou M., Golabiyan N., Synthesis and Characterization of Alumina (Al_2O_3) Nanoparticles Prepared by Simple Sol-Gel Method, *Int. J. Bio-Inorg. Hybr. Nanomater.*, **5**: 73-77 (2016).

[13] Farahmandjou M., Synthesis and Structural Study of $L1_0$- FePt nanoparticles, *Turk. J. Engin, Environ. Sci.*, **34**: 265-270 (2010).

[14] Akhtari F., Zorriasatein S., Farahmandjou M., Elahi S.M., Structural, Optical, Thermoelectrical, and Magnetic study of $Zn_{1-x}Co_xO$ ($0 \le x \le 0.10$) nanocrystals, *Int. J. Appl. Ceram. Technol.*, **15**: 723-733 (2018).

[15] Akhtari F., Zorriasatein S., Farahmandjou M., Elahi S.M., Synthesis and Optical Properties of Co^{2+}-Doped ZnO Network Prepared by New Precursors, *Mater. Res. Express.*, **5**: 065015 (2018).

[16] Khoshnevisan B., Marami M.B., Farahmandjou M., Fe^{3+}-Doped Anatase TiO_2 Study Prepared by New Sol-Gel Precursors, *Chin. Phys. Lett.*, **35**: 027501-5 (2018).

[17] Marami M.B., Farahmandjou M., Khoshnevisan B., Sol-Gel Synthesis of Fe-doped TiO2 Nanocrystals, *J. Electron. Mater.*, **47**: 3741-3749 (2018).

[18] Jafari A., Khademi S., Farahmandjou M., Nano-Crystalline Ce-doped TiO_2 Powders: Sol-Gel Synthesis and Optoelectronic Properties, *Mater. Res. Express.*, **5**: 095008 (2018).

[19] Farahmandjou M., Honarbakhsh S., Behrouzinia S., FeCo Nanorods Preparation Using New Chemical Synthesis, *J. Supercond. Nov. Magn.*, **31**: 4147–4152 (2018)

[20] Farahmandjou M., Khalili P., Study of Nano SiO_2/TiO_2 Superhydrophobic Self-Cleaning Surface Produced by Sol-Gel, *Aust. J. Basic. Appl. Sci.*, **7**: 462-465 (2013).

[21] Jurablu S., Farahmandjou M., Firoozabadi T.P., Sol-Gel Synthesis of Zinc Oxide (ZnO) Nanoparticles: Study of Structural and Optical Properties, *J. Sci. I. R. Iran.*, **26**: 281-285 (2015).

[22] Farahmandjou M., Dastpak M., Fe-Loaded CeO2 Nanosized Prepared by Simple Co-Precipitation Route, *Phys. Chem. Res.*, **6**: 713-720 (2018).

[23] Aranzabal A., Ayastuy J.L., Gonzalez J.A., Kinetics of the Catalytic Oxidation of Lean Trichloroethylene in Air Over Pd/Alumina, *Ind. Eng. Chem. Res.*, **42**: 6007-6011 (2003).

[24] Miranda B., Dı´az E., Ordon˜ez S., Dı´ez F.V., Catalytic Combustion of Trichloroethene Over Ru/Al_2O_3: Reaction Mechanism and Kinetic Study, *Catal. Commun.*, **7**: 945-949 (2006).

[25] Bejenaru N., Lancelot C., Blanchard P., Lamonier C., Rouleau L., Payen E., Dumeignil F., Royer S., Synthesis, Characterization, and Catalytic Performances of Novel Como Hydrodesulfurization Catalysts Supported on Mesoporous Aluminas, *Chem. Mater.*, **21**:522–533 (2009).

[26] Jafari A., Khademi S., Farahmandjou M., Darrudi A., Rasuli R., Structural and Optical Properties of Ce^{3+}-Doped TiO_2 Nanocrystals Prepared by Sol-Gel Precursors, *J. Electron. Mater.*, **47**: 6901–6908 (2018).

[27] Farahamndjou M., The study of Electro-Optical Properties of Nanocomposite ITO Thin Films Prepared by e-Beam Evaporation, *Rev. Mex. Fís.*, **59**: 205-207 (2013).

[28] Motaghi S., Farahmandjou M., Structural and Optoelectronic Properties of Ce-Al_2O_3 Nanoparticles Prepared by Sol-Gel Precursors, *Mater. Res. Express.*, **6**: 045008 (2019).

[29] Zarinkamar M., Farahmandjou M., Firoozabadi T.P., One-Step Synthesis of Ceria (CeO_2) Nano-Spheres by a simple Wet Chemical Method, *J. Ceram. Proc. Res.*, **17**: 166-169 (2016).

[30] Wang J.A., Bokhimi X., Morales A., Novaro O., Lo´pez T., Go´mez R., Aluminum Local Environment and Defects in the Crystalline Structure of Sol-Gel Alumina Catalyst, *J. Phys. Chem. B.*, **103**:299-303 (1999).

[31] Sohlberg K., Pennycook S.J., Pantelides S.T., Explanation of the Observed Dearth of Three-Coordinated Al on γ-Alumina Surfaces, *J. Am. Chem. Soc.*, **121**: 10999-11001 (1999).

[32] Wang H.C., Wei Y.L., Yang Y.W., Lee J.F., XAS Study of Zn-doped Al2O3 After Thermal Treatment, *J. Electron Spectrosc. Relat. Phenom.*, **144**: 817-819 (2005).

[33] Chen S., Cui X.M., Ding S.J., Novel Zn-Doped Al_2O_3 Charge Storage Medium for Light-Erasable In–Ga–Zn–O TFT Memory, *IEEE Electron Device. Lett.*, **34**: 1008-1010 (2013).

[34] Ivanova T., Harizanova A., Koutzarova T., Vertruyen B., Study of Sol-Gel Cu-doped Al_2O_3 Thin Films: Structural and Optical Properties, *J. Phys.: Conf. Ser.*, **514**: 012008 (2014).

[35] Heiba Z.K., Mohamed M.B., Wahba A.M., Imam N.G., Structural, Optical, and Electronic Characterization of Fe-doped Alumina Nanoparticles, *J. Electron. Mater.*, **47**: 711-720 (2018).

[36] Farahmandjou M., Golabiyan N., Solution Combustion Preparation of Nano-Al_2O_3: Synthesis and Characterization, *Transp. Phenom. Nano-Micro Scales.*, **3**: 100-105 (2015).

[37] Farahmandjou M., Golabiyan N., New pore structure of Nano-Alumina (Al2O3) Prepared by Sol-Gel Method, *J. Ceramic Proc. Res.*, **16**: 237-240 (2015).

[38] Huang J., Liao Q., Wang F., Huang X., Zhu H., Synthesis of Fe-doped Alumina Transparent Ceramics by co-precipitation and Vacuum Sintering, *Ceram. Int.*, **44**: 799-804 (2018).

[39] Heiba Z., Mohamed M.B., Wahba A.M., Imam N.G., Structural, Optical, and Electronic Characterization of Fe-doped Alumina Nanoparticles, *J. Electron. Mater.*, **47**: 711-720 (2018).

[40] Scherrer P., Bestimmung der Grosse und der Inneren Struktur von Kolloidteilchen Mittels Rontgenstrahlen, Nachrichten von der Gesellschaft der Wissenschaften, *Gottingen. Mathematisch-Physikalische Klasse*., **2**: 98-100 (1918).

[41] Hafshejani L.D., S., Koponen H., Riikonen J., Karhunen T., Tapper U., Lehto V.P., Moazed H., Naseri A., Hooshmand A., Jokiniemi J., Bhatnagar A., Lähde A., Synthesis and Characterization of Al_2O_3 nanoparticles by Flame Spray Pyrolysis (FSP) — Role of Fe Ions in the Precursor, *Powder Technol.*, **298**: 42-49 (2016).

[42] Marami M.B, Farahmandjou M., Water-Based Sol-Gel Synthesis of Ce-Doped TiO2 Nanoparticles, *J. Electron. Mater.*, **48**: 4740-4747 (2019).

[43] Farahmandjou M., Soflaee F., Synthesis of Iron Oxide Nanoparticles using Borohydride Reduction, *Int. J. Bio-Inorg. Hybr. Nanomater.*, **3**: 203-206 (2014).

[44] Farahmandjou M., Salehizadeh S.A., The Optical Band Gap and the Tailing States Determination in Glasses of TeO_2-V_2O_5-K_2O System, *Glass Phys. Chem.*, **39**: 473-479 (2013).

[45] Honarbakhsh S., Farahmandjou M., Behroozinia S., Synthesis and Characterization of Iron-Cobalt (FeCo) Nanorods Prepared by Simple Co-precipitation Method, *J. Fund. Appl. Sci.*, **8**: 892-900 (2016).

[46] Behrouzinia S., Salehinia D., Khorasani K., Farahmandjou M., The Continuous Control of Output Power of a CuBr Laser by a Pulsed External Magnetic Field, *Opt. Commun.*, **436**: 143-145 (2019).

[47] Farahmandjou M., Motaghi S., Sol-gel Synthesis of Ce-doped α-Al_2O_3: Study of Crystal and Optoelectronic Properties, *Opt. Commun.*, **441**: 1-7 (2019).

[48] Khodadadi A., Farahmandjou M., Yaghoubi M., Investigation on Synthesis and Characterization of Fe-doped Al2O3 Nanocrystals by New Sol-Gel Precursors, *Mater. Res. Express.*, **6**: 025029 (2019).

[49] Sebt S.A., Parhizgar S.S., Farahmandjou M., Aberomand P., Akhavan M., The Role of Ligands in the Synthesis of FePt Nanoparticles, *J. Supercond. Nov. Magn.*, **22**: 849-854 (2009).

[50] Khodadadi A., Farahmandjou M., Yaghoubi A., Amani R., Structural and Optical Study of Fe3+-Doped Al2O3 Nanocrystals Prepared by New Sol-Gel Precursors, *Int. J. Appl. Ceram. Technol.*, **16**: 718-726 (2018).

[51] Ramazani M., Farahmandjou M., Firoozabadi T.P., Effect of Nitric Acid on Particle Morphology of the Nano-TiO_2, *Int. J. Nanosci. Nanotech.*, **11**: 115-122 (2015).

[52] Farahmandjou M., Zarinkamar M., Synthesis of Nano-Sized Ceria (CeO2) Particles Via A Cerium Hydroxy Carbonate Precursor and the Effect of Reaction Temperature on Particle Morphology, *J. Ultrafine Grained Nanostruct. Mater.*, **48**: 5-10 (2015).

[53] Farahmandjou M., Sebt S.A., Parhizgar S.S., Aberomand P., Akhavan M., Stability Investigation of Colloidal Fept Nanoparticle Systems by Spectrophotometer Analysis, *Chin. Phys. Lett.*, **26**: 027501-3 (2009).

[54] Farahmandjou M., Zarinkamar M., Firoozabadi T.P., Synthesis of Cerium Oxide (CeO2) Nanoparticles Using Simple CO-Precipitation Method, *Rev. Mex. Fís.*, **62:** 496-499 (2016).

[55] Farahmandjou M., Effect of Oleic Acid and Oleylamine Surfactants on the Size of FePt Nanoparticles, *J. Supercond. Nov. Magn.*, **25**: 2075-2079 (2012).

[56] Khatoon S., Wani I.A., Ahmed J., Magdaleno T., Al-Hartomy O.A., Ahmad T., Effect of High Manganese Substitution At ZnO Host Lattice Using Solvothermal Method: Structural Characterization and Properties, *Mater. Chem. Phys.*, **138**: 519-528 (2013).

[57] Kumar S., Kumar R., Singh D.P., Swift Heavy Ion Induced Modifications in Cobalt Doped ZnO Thin Films: Structural and Optical Studies, *Appl. Surf. Sci.*, **255:** 8014-8018 (2009).